

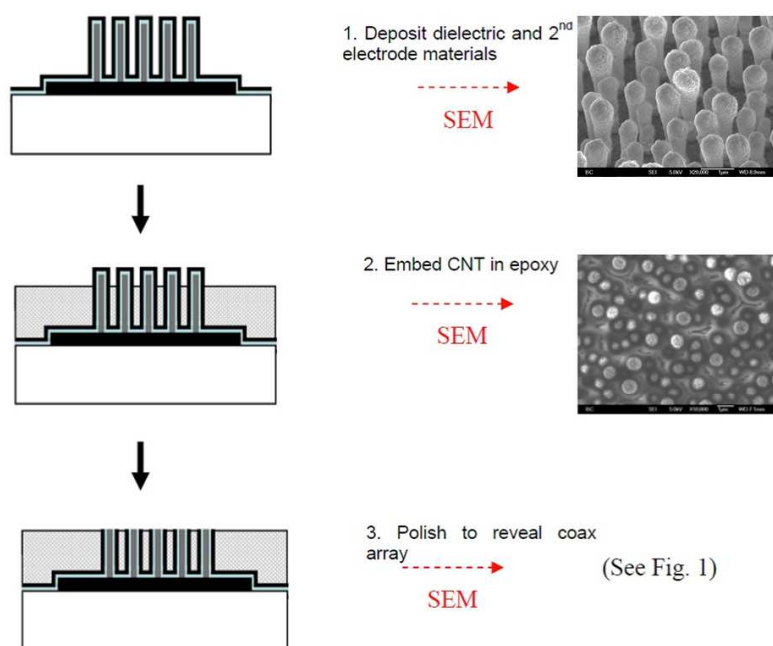
Ultrasensitive chemical detection using a nanocoax sensor

Huaizhou Zhao^{‡,§}, Binod Rizal[‡], Gregory McMahon[‡], Hengzhi Wang[‡], Pashupati Dhakal[‡], Timothy Kirkpatrick[‡], Zhifeng Ren[‡], Thomas C. Chiles[§], Michael J. Naughton^{‡,*} and Dong Cai^{§*}

[‡]Department of Physics, [§]Department of Biology
Boston College, Chestnut Hill, Massachusetts 02467, U.S.A

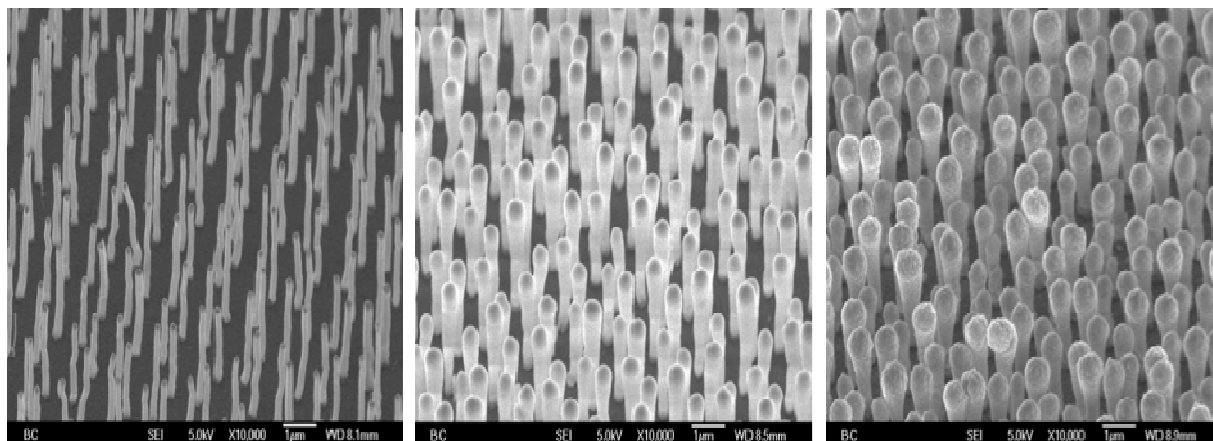
*Correspondence should be addressed: naughton@bc.edu; caid@bc.edu

Supporting Information



Scheme 1S. Fabrication of nanocoaxial cavity array.

Figure S1(a). Fabrication scheme



CNTs

+ 10 nm ALD Al_2O_3 and
150 nm sputtered Al_2O_3

+ 250 nm Al outer layer

Figure S1(b). SEM images for each step of fabrication process

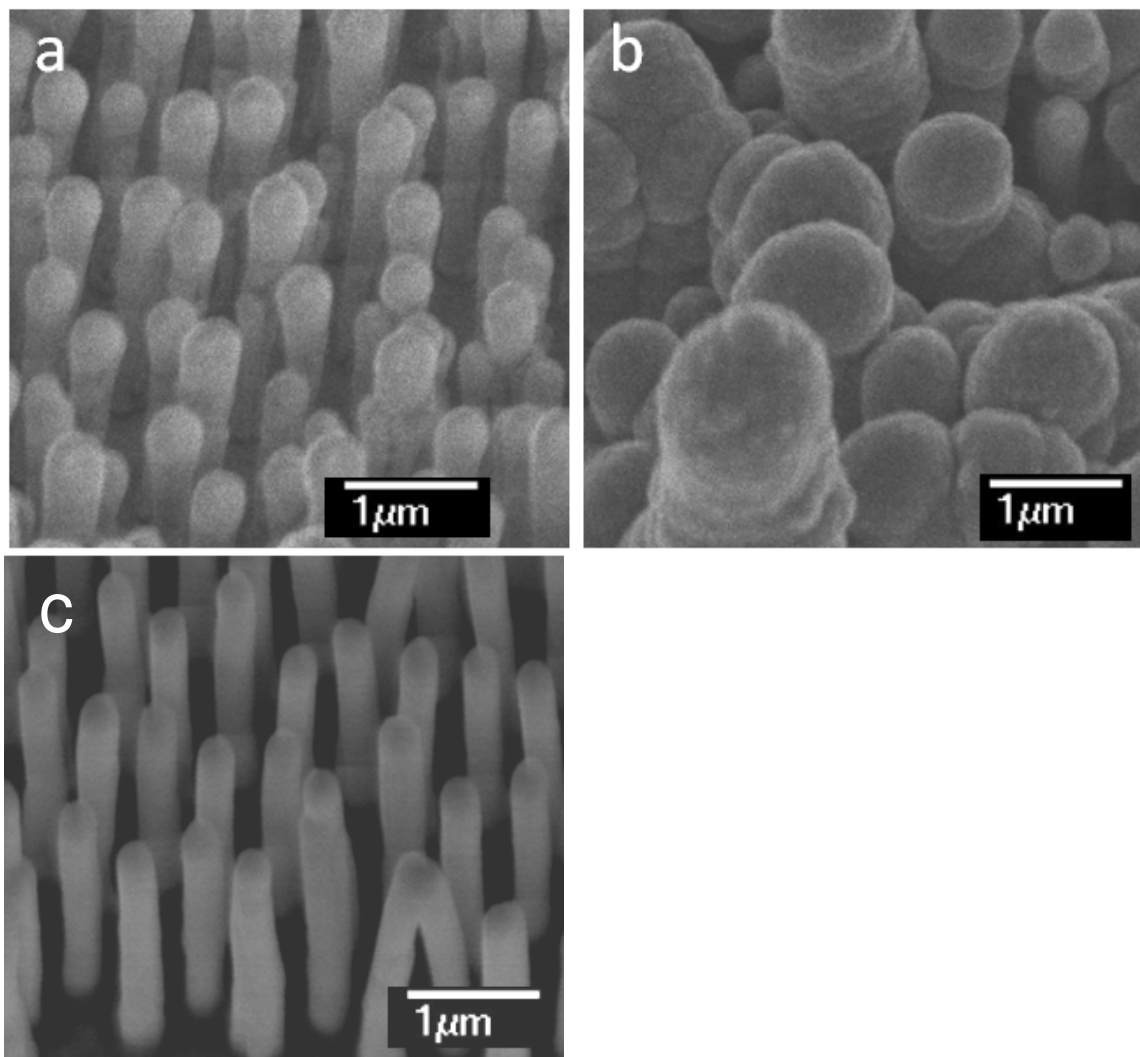


Figure S2. Electropolymerization of PPy on Al₂O₃-coated CNT arrays. For Al₂O₃ from sputter deposition, (a) and (b) correspond to the SEM images before and after PPy electropolymerization, respectively. No apparent PPy deposition was shown on the ALD Al₂O₃ (80 nm) coated CNT array (c).

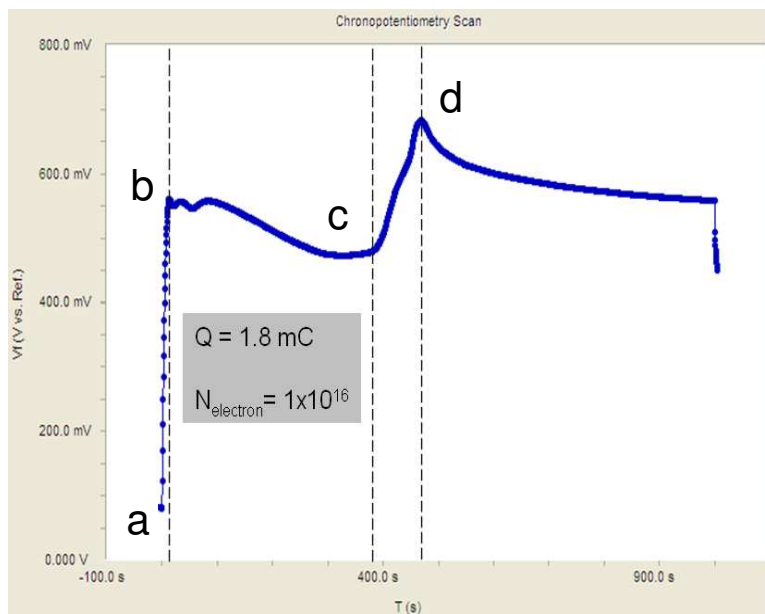


Figure S3. The phases of galvanostatic deposition of PPy in porous Al₂O₃ thin film. a-b: PPy nucleated at the pore bottom of Al₂O₃; b-c: PPy grew inside the pores; c-d: the transition phase; d: PPy deposited outside the Al₂O₃ coating.

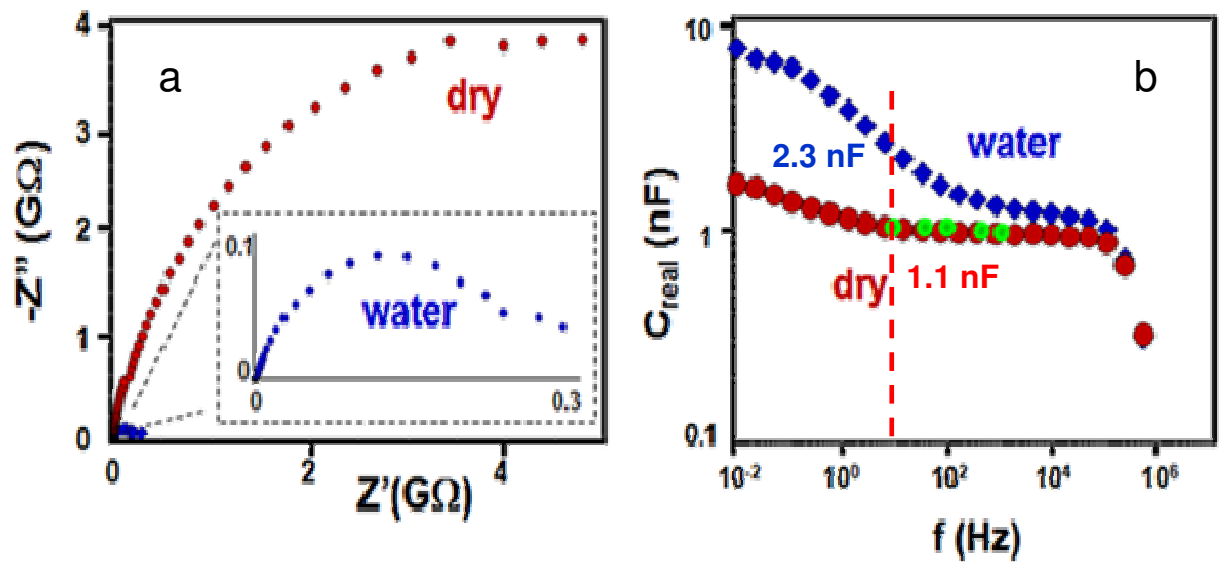


Figure S4. Measurement of sensor capacitance with impedance spectroscopy. a: Nyquist plots of impedance spectroscopy from 10 mHz to 1 MHz for dry (red) and water-immersed (blue) sensor. b: Capacitance extracted from data shown in a. Green symbols refer to the capacitance measurement by lock-in amplifier, showing consistency with that extracted from spectroscopy.

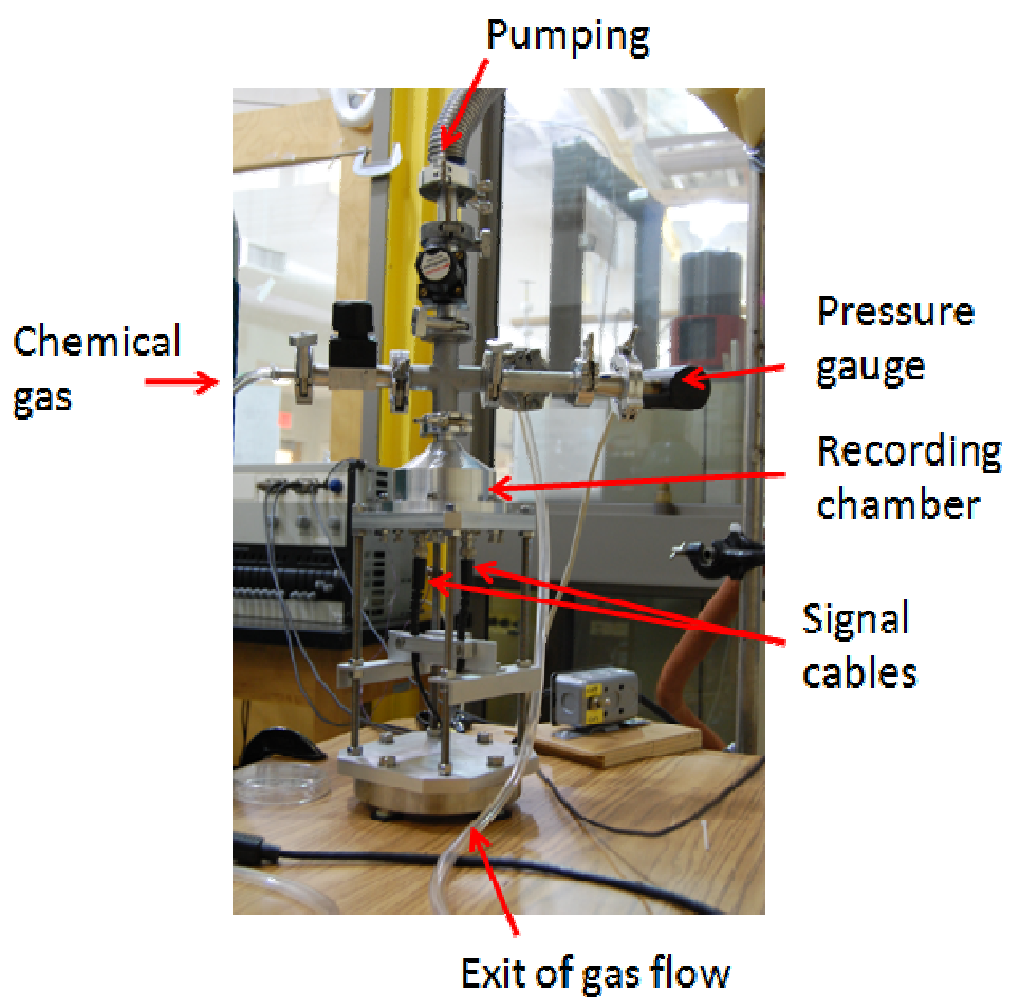
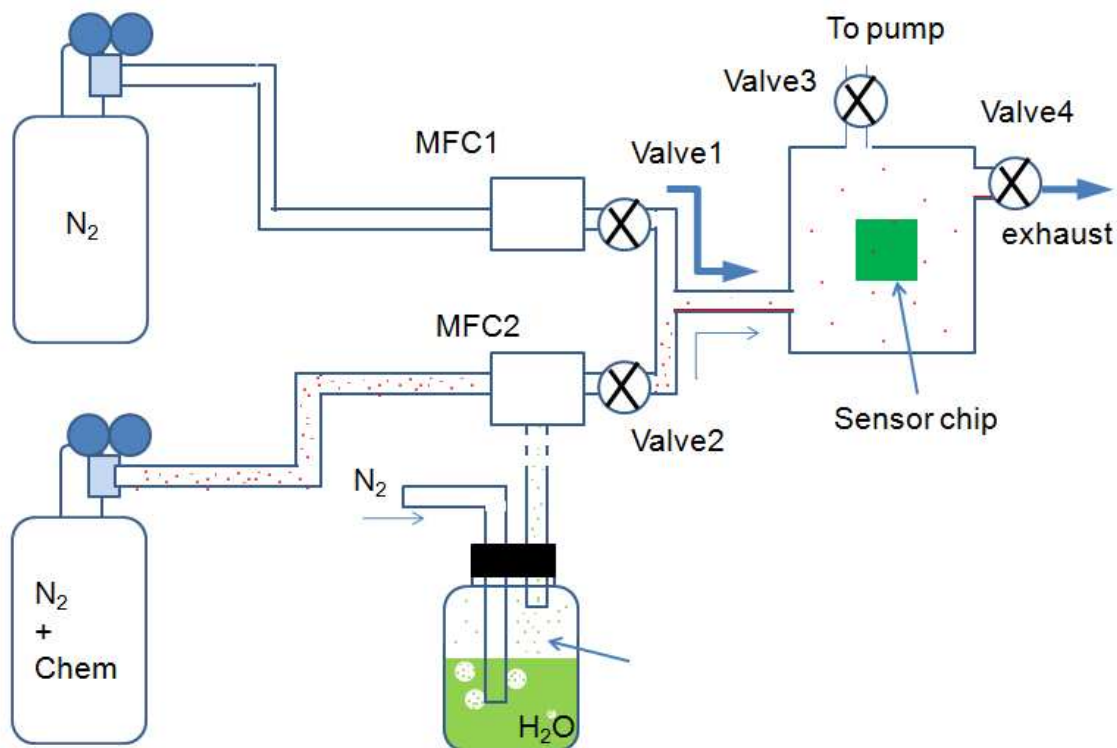


Figure S5. The measurement chamber.



Scheme S6. The gas dilution system.

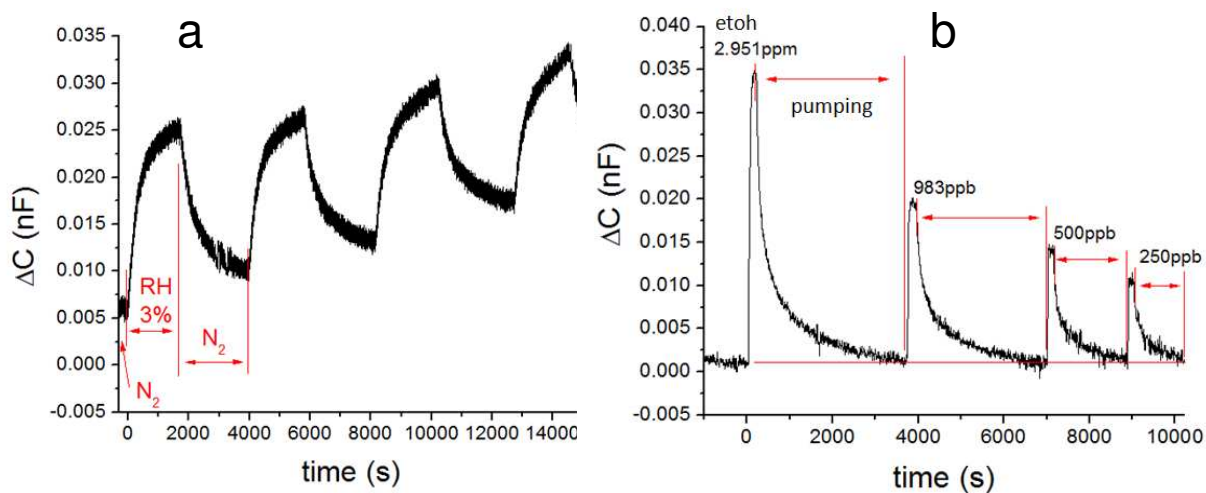


Figure S7. Sensor response to RH and ethanol. a: Sensor was treated with humidified N_2 gas at $RH=3\%$ and flushed with N_2 gas four times. b: Response to a series of ethanol concentrations. The ethanol vapor carried by N_2 gas is applied to the sensor after evacuation with pumping. The recovery (desorption) takes tens of times longer than the rising (adsorption) phase.

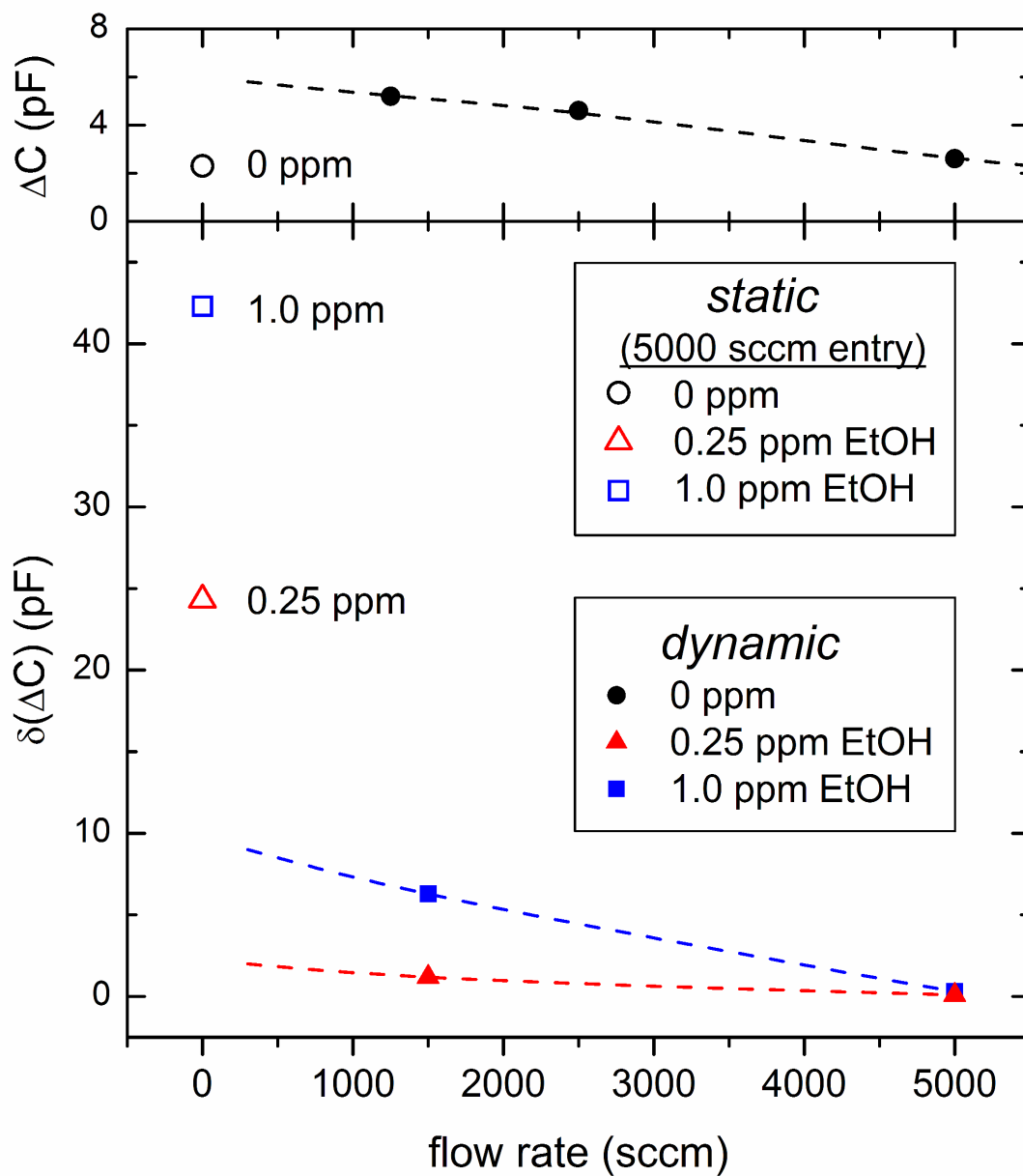


Figure S8. Flow rate dependence of sensitivity for pure nitrogen and ethanol at 0.25 ppm and 1.0 ppm concentrations in N_2 , under dynamic and static measurement conditions, showing considerably higher sensitivity for the latter.